

High Voltage DC Transmission 2

1.0 Introduction

Interconnecting HVDC within an AC system requires conversion from AC to DC and inversion from DC to AC. We refer to the circuits which provide conversion from AC to DC as *rectifiers* and the circuits which provide conversion from DC to AC as *inverters*. The term *converter* is used to generically refer to both rectifiers and inverters.

Converter technologies are based on use of switching devices collectively referred to in the HVDC community as *valves*. Valves may be non-controlled or controlled. A non-controlled valve behaves as a diode, appearing as

- a closed switch when forward-biased (voltage is positive), resulting in the device being “on”;
- an open switch when reverse-biased (voltage is negative), resulting in the device being “off.”

A controlled valve has a similar characteristic except it requires a gate pulse to turn on, i.e., it appears as

- a closed switch when forward-biased (voltage is positive) AND the gate is pulsed, resulting in the device being “on”
- an open switch when reverse-biased (voltage is negative), resulting in the device being “off.”

A thyristor (also known as silicon-controlled rectifiers or SCRs) is a type of controlled valve. Figure 1 illustrates the difference in current-voltage characteristics between a diode and a thyristor; notice the anode (A) and cathode (K). Observe that the diode is a two-terminal device whereas the thyristor is a three-terminal device.

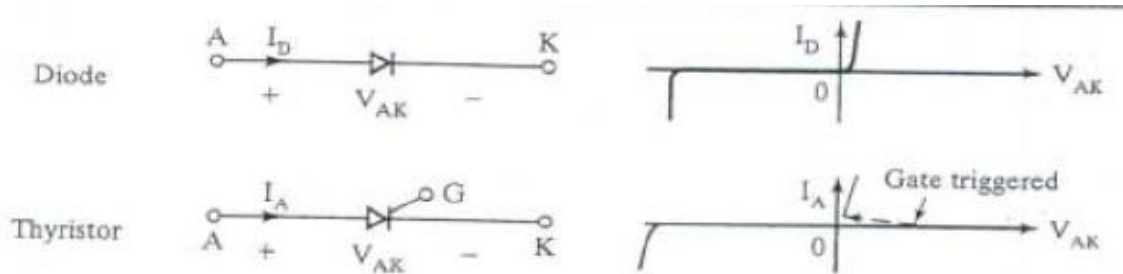


Fig. 1

There have been 3 types of devices for implementing HVDC converter circuits: mercury-arc, thyristors, and insulated gate bipolar transistors (IGBTs).

Mercury-arc devices were developed in the early 1900's and used for the first time within an HVDC installation in 1932. All HVDC installations built between then and about 1972 used mercury-arc devices. The last HVDC installation using mercury-arc devices was built in 1975. A link between the North and South islands of New Zealand, decommissioned in 2012, was the last HVDC installation in operation using mercury arc valves.

We discuss thyristor-based converters in Section 2 and IGBT-based converters in Section 3.

2.0 Thyristor-based converters

A so-called 6-pulse three phase rectifier is shown in Fig. 2. The circuit of Fig. 2a employs a Y-connected, three-phase source $v_i(\omega t)$, delivering dc output v_o to resistive load through a bridge consisting of six controlled switches. It performs six switching operations per period and hence is called a 6-pulse converter. Analysis is provided below (also given in [1, ch2] and other texts).

The operation of the scheme can be understood based on the following observations:

1. Exactly two thyristors are conducting at any moment, as can be seen from the bottom of Fig. 2c. One will be from upper group (1, 3, 5) and one from lower group (2, 4, 6).
 - Th1 is fired at $\omega t = \alpha$ and then left on for 60° , after which a thyristor is fired every 60° thereafter (gate pulse need not be sustained to maintain thyristor on-state).
 - At firing angle, we want to be “on” the pair of thyristors that give the most positive line-to-line voltage. We determine the thyristor pair that should be on by (a) identifying the most positive line-to-line voltage; (b) inspecting the circuit and identifying thyristors that need to be on to place the most positive line-to-line voltage (as identified in (a)) across the load.
2. Thyristors commutate (turn off) when they become reversed biased. This occurs whenever the cathode voltage exceeds the anode voltage.

At $\omega t = \alpha - \pi/3$ (corresponding to “view 1” in the figure),

- v_{cb} is the most positive voltage relative to other line-to-line voltages;
- Th 5, 6 should be on;
- At $\pi/3$ later ($\omega t = \alpha$), we turn on Th 1 to apply v_{ab} across the load;
- At $\omega t = \pi/3$, v_{ca} goes negative (also indicated in Fig. 2b by v_{ac} going positive) and when Th1 is fired (at $\omega t = \alpha$), Th5 is reverse biased, and it commutates (turns off). This is also seen in that at this time, v_{ab} goes higher than v_{cb} , and so when Th1 turns on, node “a” has higher potential than node “c,” so Th5 reverse biases & turns off.

At $\omega t = \alpha$,

- v_{ab} is the most positive voltage relative to other line-to-line voltages;
- Th 1, 6 should be on;
- At $\pi/3$ later ($\omega t = \alpha + \pi/3$), we turn on Th2 to apply v_{ac} across the load;
- At $\omega t = 2\pi/3$, v_{cb} goes negative (also indicated in Fig. 2b by v_{bc} going positive) and when Th2 is fired (at $\omega t = \alpha + \pi/3$), Th6 is reverse biased, and it commutates (turns off). This is also seen in that at this time, v_{ac} goes higher than v_{ab} , and so when Th2 turns on, node “b” has higher potential than node “c,” so Th6 reverse biases and turns off.

When do thyristors commute?

Thyristors commute (turn off) when they become reverse biased. This occurs whenever the cathode voltage exceeds the anode voltage.

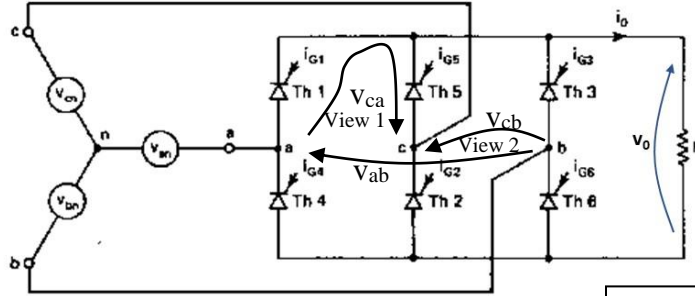
The first commutation:

(see figs a and b).

Initially, Th5, Th6 are on.

View 1: v_{ca} (thick curve) goes neg at this moment (equivalent to v_{ac} going positive) and when Th1 is fired (later, at $\omega t = \alpha$), Th5 is reverse biased, and it turns off.

View 2: v_{ab} goes higher than v_{cb} (circle), and so when Th1 turns on (later, at $\omega t = \alpha$), node "a" has higher potential than node "c," so Th5 reverse biases & turns off.

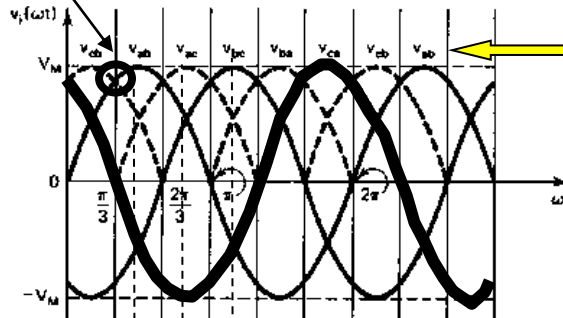


← One from upper group.

Exactly 2 thyristor are on at any moment.

← One from lower group.

(a) Circuit schematic



(b) Balanced, three-phase input source

How to know which thyristors to turn on?

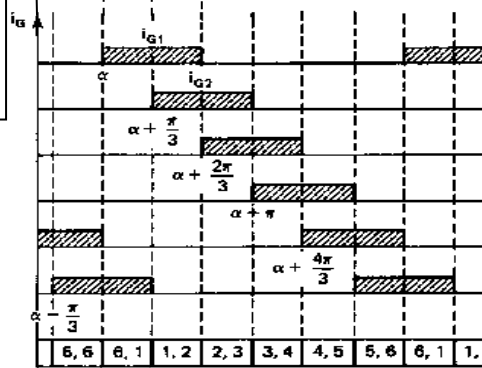
At firing angle, we turn on the pair of thyristors giving most positive line-to-line voltage. We can determine the thyristor pair that should be on by (a) identifying the most positive line-to-line voltage; (b) inspecting the ckt & identifying the thyristors that need to be on to place the most positive line-to-line voltage (as identified in (a)) across the load.

First period: v_{cb} is most positive l-l voltage, so node c needs to be at pos load terminal (Th5 on); node b at neg load terminal (Th6 on).

Second period: v_{cb} is most positive l-l voltage, so node c needs to be at pos load terminal (Th5 on); node b at neg load terminal (Th6 on).

...

Th1 is fired at firing angle $\omega t = \alpha$, then left on for 60° , after which a thyristor is fired every 60° thereafter, in following order: Th2, Th3, Th4, Th5, Th6, Th1, ...



← This shaded area indicates time when Th1 is on.

← This shaded area indicates time when Th2 is on.

← This shaded area indicates time when Th3 is on.

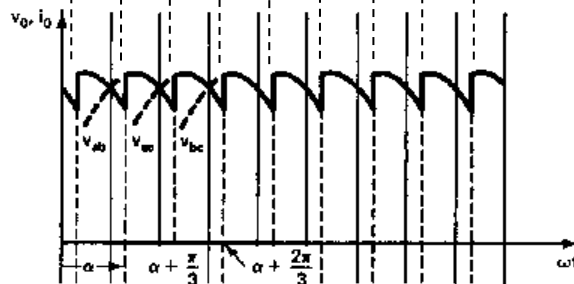
⋮

⋮

⋮

Exactly 2 thyristors are on at any moment. 6 switching operations per period with thyristors on following each operation as: [5,6], [6,1], [1,2], [2,3], [3,4], [4,5]...

(c) Gate pulses and thyristor conduction sequence



(d) Output signal waveforms

Fig. 2: Three-phase, full-wave controlled rectifier scheme

Inspection of v_o shows that its fundamental frequency of variation is six times that of the input source (6 cycles of the new waveform to every one cycle of the 60Hz waveform). So the harmonic of the output voltage will be multiple orders of 6.

With the period of the output voltage being $2\pi/6 = \pi/3$, the average value of $v_o = V_{dc}$ is given by:

$$\begin{aligned}
 V_{dc} &= \frac{1}{T} \int_{\text{1 period}} v_o(\omega t) d(\omega t) \\
 V_{dc} &= \frac{3}{\pi} \int_{\alpha+(\pi/3)}^{\alpha+(2\pi/3)} v_o(\omega t) d(\omega t) = \frac{3}{\pi} \int_{\alpha+(\pi/3)}^{\alpha+(2\pi/3)} v_{ab}(\omega t) d(\omega t) \quad (1) \\
 &= \frac{3}{\pi} \int_{\alpha+(\pi/3)}^{\alpha+(2\pi/3)} V_M \sin(\omega t) d(\omega t) = \frac{3V_M}{\pi} \cos\alpha
 \end{aligned}$$

where V_M is the maximum line-to-line voltage. Observe (a) the integration is performed over the second interval of Fig. 2b (where the voltage is v_{ab}); (b) following integration, we evaluated using the identity $\cos(x+y) = \cos x \cos y - \sin x \sin y$.

Similarly, the rms value of the load voltage is:

$$V_{\text{rms}} = \left[\frac{3}{\pi} \int_{\alpha+(\pi/3)}^{\alpha+(2\pi/3)} v_o^2 d(\omega t) \right]^{1/2} = V_M \left[\frac{1}{2} + \frac{3\sqrt{3}}{4\pi} \cos(2\alpha) \right]^{1/2} \quad (2)$$

The DC voltage and the rms voltage are close, but not the same; for example, at $\alpha=0$, we obtain:

$$V_{dc} = \frac{3V_M}{\pi} \cos 0 = \frac{3V_M}{\pi}$$

$$V_{rms} = V_M \left[\frac{1}{2} + \frac{3\sqrt{3}}{4\pi} \cos(0) \right]^{1/2} = \frac{3V_M}{\pi} \left[\frac{2\pi + 3\sqrt{3}}{12} \right] = \frac{3V_M}{\pi} (0.9563)$$

The DC voltage is often used as a proxy to compute power; in reality, however, this gives the so-called “DC Power” which is not the same as the “average power” obtained from the rms values. Although DC quantities for voltages and currents are often obtained for power electronic circuits, their use for power calculations should always be seen to be approximations at best [2, pg. 40].

Fig. X illustrates the output voltage waveform of the converter for different values of firing angle α .

- In the first two figures of Fig. X, voltage and currents are positive (current flow into the load of Fig. 2a),
- In the third and fourth figures (towards the bottom) of Fig. X, the voltages are negative, whereas the current must still be positive (current reversal is not possible for the thyristor-based converter since thyristors are unidirectional devices).

It is important to understand that the only control variable distinguishing the curves of Fig. X is firing angle.

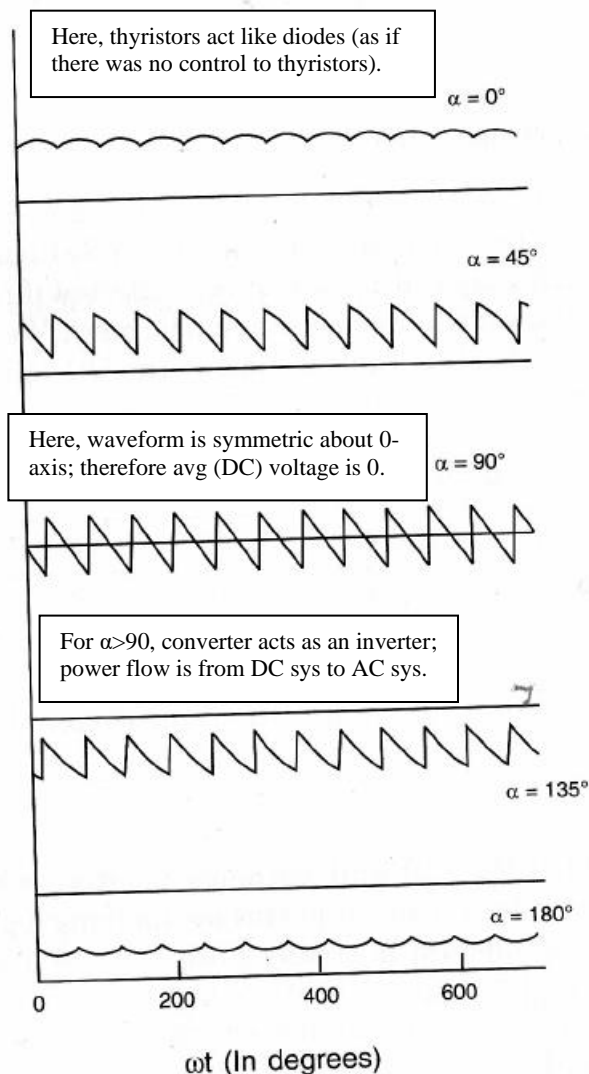


Fig. X

This arrangement is realized for HVDC rectifier circuits using a transformer, illustrated in Fig. 3 [3]. It is typical that the AC voltage input would be stepped down through a transformer before applying it to the converter.

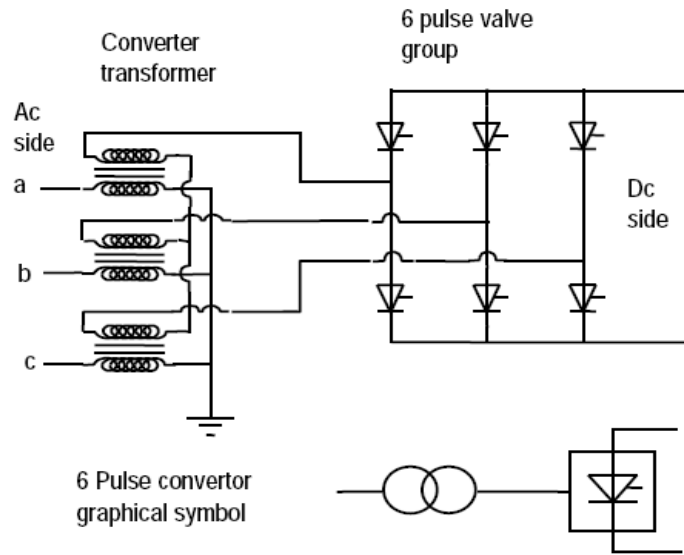


Fig. 3

The drawing at the bottom of Fig. 3 is a shorthand way of communicating the 6-pulse arrangement shown in the top of Fig. 3.

Mercury-arc converters were 6-pulse, but almost all thyristor-based converters developed recently have been 12-pulse. A 12-pulse converter, which fires a thyristor every 30° , is at left in Fig. 4. Its shorthand circuit symbol is at right. The basic building block for the 12-pulse converter is the 6-pulse converter.

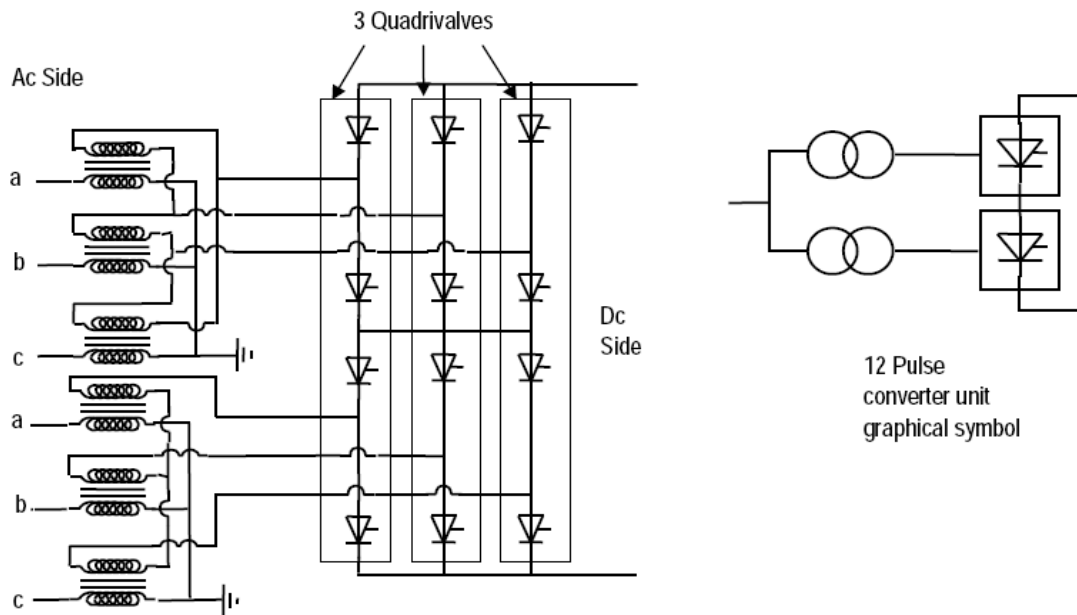


Fig. 4

We make three observations regarding Fig. 4.

- The two 6-pulse bridges are connected in series to increase the DC voltage.
- Because each thyristor is rated at only a few kV, handling the high levels of AC voltages may require stacking several thyristors in series to form a single valve.
- Packaging may be done in units of 1 valve, 2 valves or 4. A group of 4 valves (a single vertical stack in Fig. 4), assembled as one valve structure by stacking four valves in series, is referred to as a “quadrivalve.” A $\pm 500\text{kV}$ quadrivalve may have hundreds of thyristors stacked in series [3].
- The two transformers on the AC side are both fed from the same three-phase AC source; however, to obtain 12 pulses that are symmetrically phase-

displaced by 30° , one transformer (the bottom one) is connected Y-Y and the other Y- Δ , so that the

- line to line voltages of the Δ -connected secondary (which are in-phase with the line to neutral voltages of the primary side)
- are 30° behind the line to line voltages of the Y-connected secondary.

By taking appropriate polarities, one can obtain voltages that are phase displaced from one another by consecutive 30° , as shown in Fig. 5 (dotted lines are polarity reversals). Equal amplitudes are obtained using transformers of appropriate winding ratios.

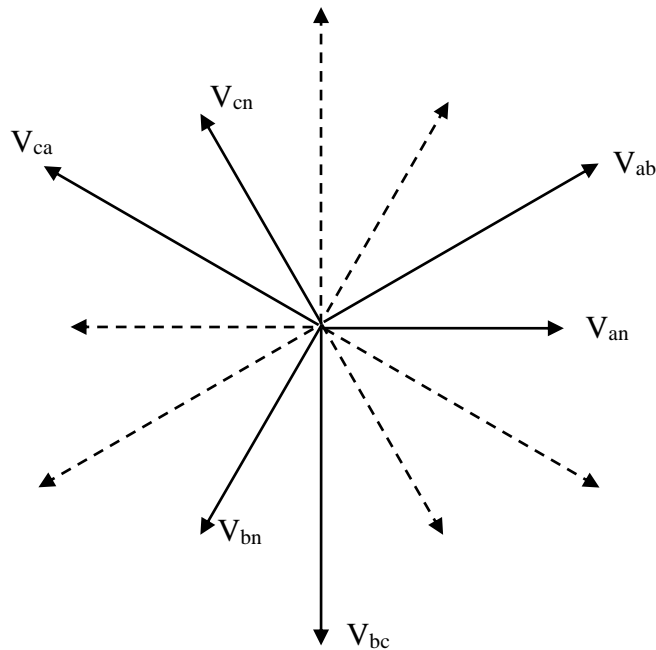


Fig. 5

DC voltage control is obtained by controlling either the magnitude of the applied AC voltage V_m or the firing angle α .

For values of firing angle $0 < \alpha < 90$, $V_{dc} > 0$, but for $90 < \alpha < 180$, $V_{dc} < 0$. Therefore inversion (necessary for the negative pole) is achieved using $90 < \alpha < 180$. To differentiate between rectifier and inverter operation, the extinction angle $\beta = \pi - \alpha$ is defined.

Figure 6a [3] illustrates rectifier and inverter operation. Some comments about Fig. 6 follow:

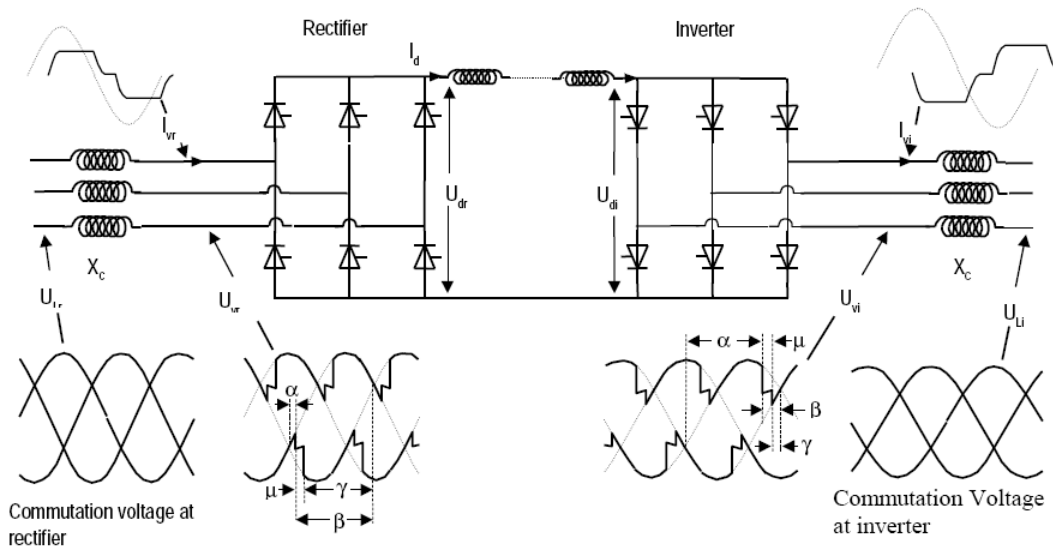


Fig. 6a

- The overlap angle μ is indicated in Fig. 6 and accounts for the finite turn-on and turn-off time of each switching operating when there will be some overlap between thyristor on-states. We ignore this in the ideal case.

- Commutation at the inverter side occurs as a result of the action of the three-phase AC voltage at the inverter, similar to the rectifier side.
- Due to the line commutation valve switching process, a non-sinusoidal current is taken from the A.C. system at the rectifier (I_{vr} in Fig. 6) and is delivered to the A.C. system at the inverter (I_{vi} in Fig 6). Both I_{vr} and I_{vi} are lagging to the alternating voltage and therefore both terminals absorb reactive power and usually require capacitive shunt compensation.
- Reversal of power flow is accomplished by changing the polarity of the DC voltage. Such dual operation of the converter bridges as either a rectifier or inverter is achieved through firing control of the grid pulses [3].

Some other attributes for thyristor-based HVDC are illustrated in Fig. 6b.

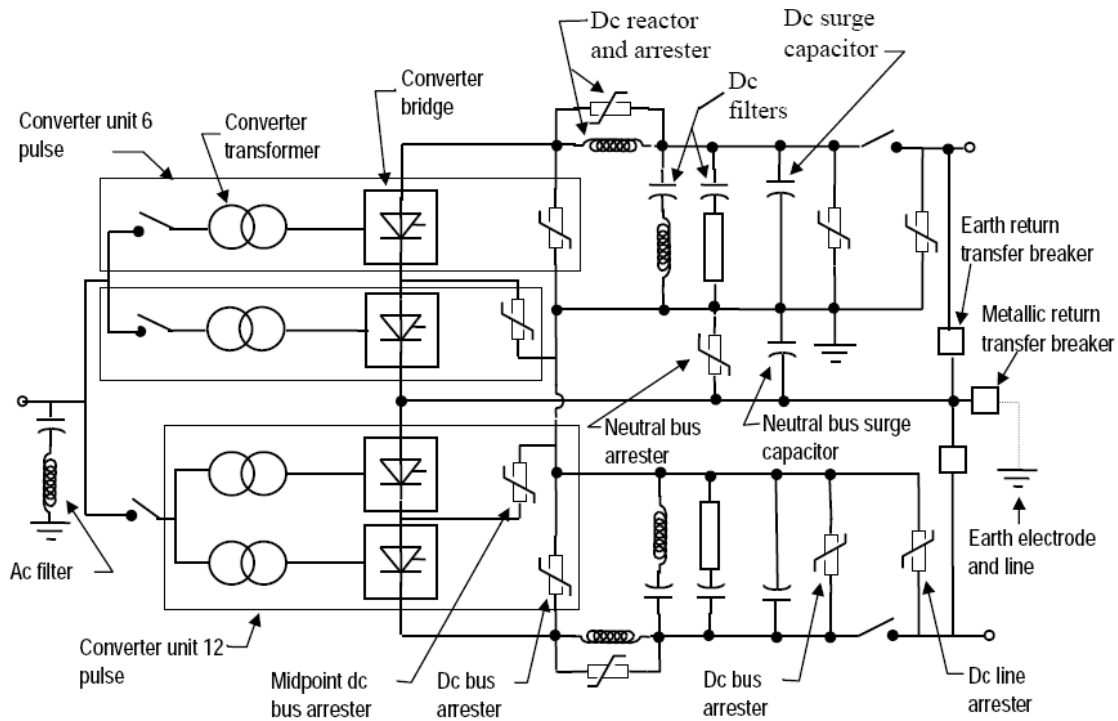


Fig. 6b

Of particular interest, we note the following:

- **AC filters:** Converter operation results in AC current harmonics, and these must be filtered. The characteristic AC side current harmonics generated by 12 pulse converters are $12n \pm 1$ where n equals all positive integers. AC filters are typically tuned to 11th, 13th, 23rd and 25th harmonics for 12 pulse converters [3]. See Section 5.0 for related analysis.
- **High-frequency filters:** The converter operation also results in very high frequency distortion which will propagate into the AC system if not filtered.
- **DC smoothing:** The function of the smoothing reactor on the DC side is to reduce the current ripple caused by the non-smooth DC voltage.

- DC Filter: There are sinusoidal AC harmonics superimposed on the DC terminal voltage. This AC harmonic component on the DC line can link with conductors used in communication systems, inducing harmonic current flow in them.
- Surge arresters across each valve in the converter bridge, across each converter bridge and in the d.c. and a.c. switchyard are coordinated to protect the equipment from all overvoltages regardless of their source.

3.0 IGBTs

The thyristor is a single-component device, i.e., it is comprised of a single solid-state device. The insulated gate bipolar transistor (IGBT) is different in that it is a *hybrid device* which is a device comprised of two or more solid state devices. Specifically, the IGBT combines a MOSFET with a BJT as illustrated in Fig. 7.

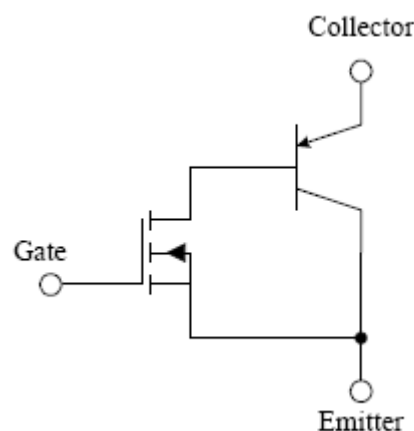


Fig. 7

The circuit symbol for the IGBT is given in Fig. 8 together with the operating characteristic.

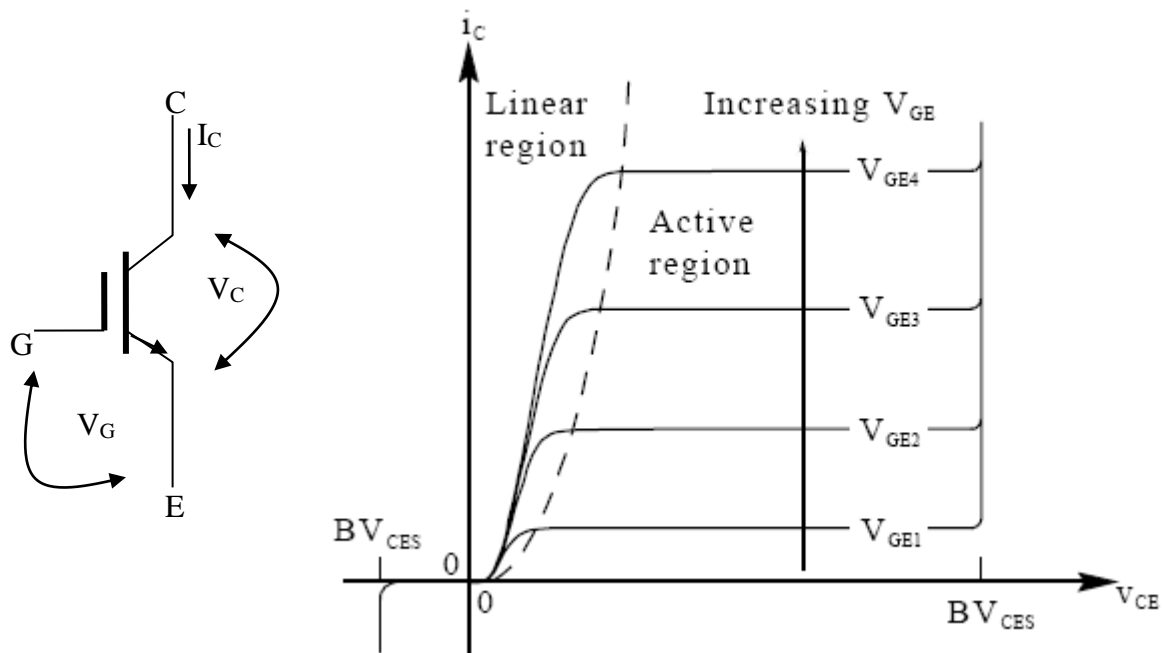


Fig. 8

The IGBT operates as a switch by operating between the active region and its cutoff region.

Figure 9a [] and Figure 9b [4] illustrate the difference between IGBTs and thyristors in terms of switching speed and power handling capabilities. Although the numbers may have changed since these figures were created, the basic features have not:

➔ Thyristor-based converters have significantly higher power handling capability than do IGBT-based converters.

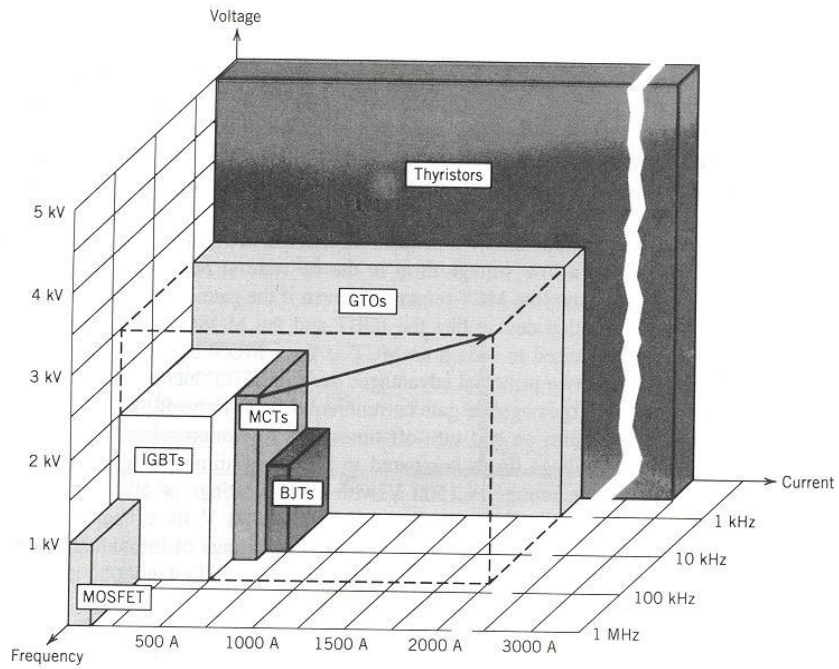


Fig.9a

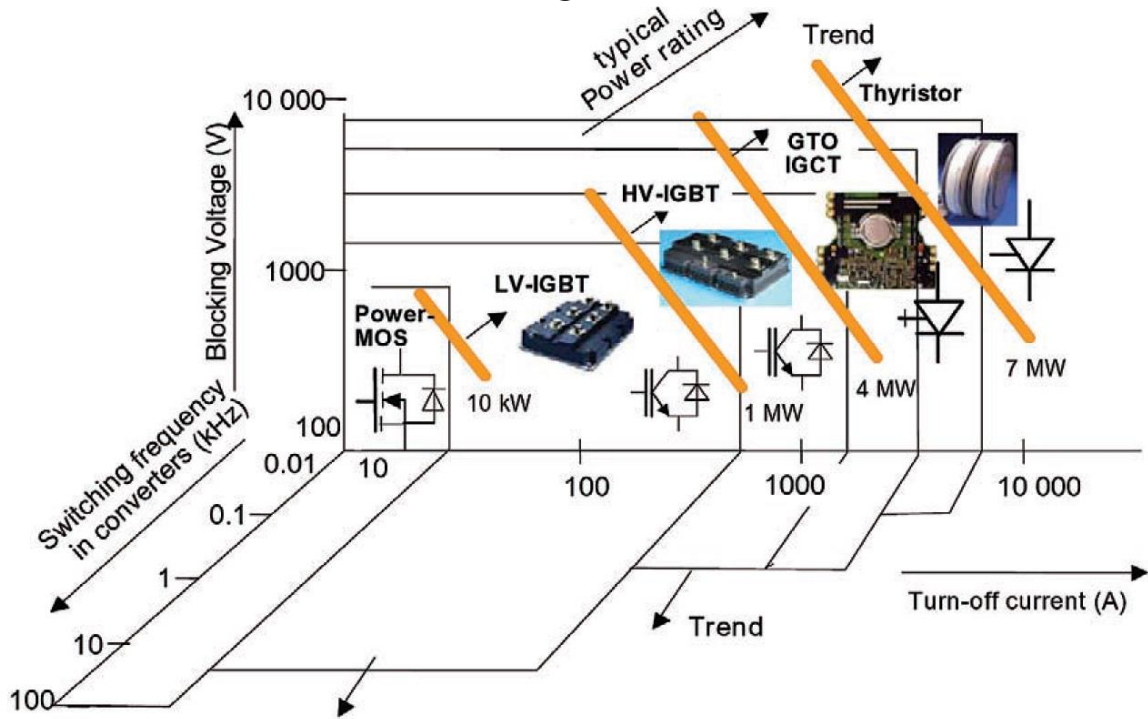


Fig. 9b

For application to converters used in HVDC applications, an antiparallel diode is integrated in the same IGBT semiconductor package to ensure current capability in the reverse direction, thus making the device a reverse-conducting switch. Figure 9c illustrates an IGBT with an antiparallel diode. The package of IGBT with antiparallel diode is referred to as a *switch cell* [5].

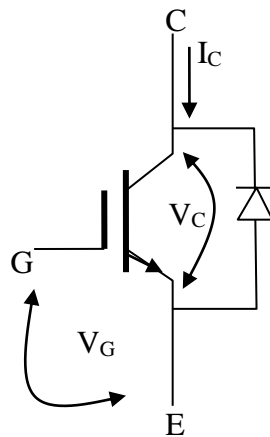


Fig. 9c

4.0 Voltage source converters

The 6-pulse and 12-pulse Line Commutated Converter (LCC) we described in Section 2.0 of these notes are of a converter family called *current source converters* (CSC). The CSC maintains constant directionality of the DC-side current, and so, to change the direction of average power flow, we must change the polarity of the DC-side voltage [5].

As indicated in Figs. 6a and 6b, the DC-side of a CSC is in series with a large inductor to smooth the current and maintain its continuity, making the DC-side appear like a current source. This happens because the change in inductor current must be limited to maintain finite voltages, as indicated by

$$\frac{di}{dt} = \frac{1}{L} v(t)$$

Another class of converters is referred to as the *voltage source converter* (VSC). The VSC maintains constant directionality of the DC-side voltage, and so, to change the direction of average power flow, we must change the polarity of the DC-side current [5].

As indicated in Fig. 9d, the DC-side of a VSC is in parallel with a large capacitor to smooth the voltage and maintain its continuity, making the DC-side appear like a voltage source. This happens because the change in capacitor voltage must be limited to maintain finite currents, as indicated by

$$\frac{dv}{dt} = \frac{1}{C} i(t)$$

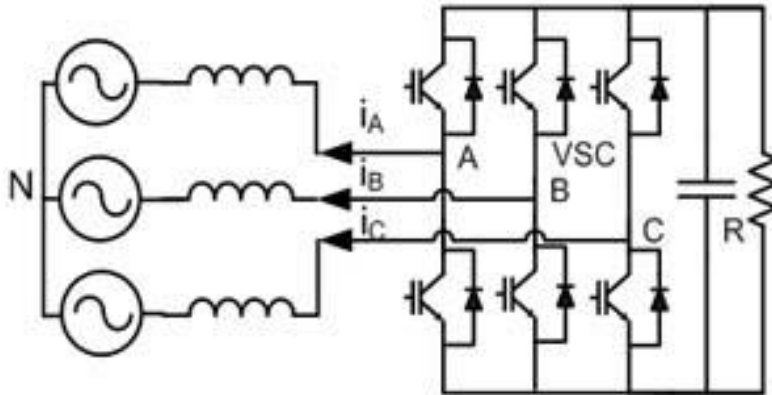


Fig. 9d

The IGBT (or in some cases, the GTO) is used in voltage source converter (VSC) HVDC applications, and was introduced in the late 1990's. A critical difference between VSC-based HVDC and thyristor-based HVDC is that whereas thyristor-based HVDC is line-commutated (switched off when the thyristor is reverse biased from the AC voltage), the VSC-based HVDC is forced commutated via control circuits driven by pulse-width modulation (PWM).

Thus, we see that

- thyristor control is only for turning *on* the device; it is then turned *off* by the circuit (or the “line”); thus, converters that use them are referred to as *line-commutated converters* (LCCs).
- IGBT control is for turning the device *on* and *off*; converters that utilize IGBTs are referred to as *forced commutated converters* (FCCs) or *self-commutated converters* (SCCs).

The ability for IGBTs to both turn on and turn off via control signals enable VSCs to have control capability that is not available with thyristors.

In particular, in an LCC, the current at both rectifier and inverter terminals is lagging, and therefore both terminals draw reactive power. This is because of the line commutation; the current initiation in each SCR can only be delayed with respect to the zero crossing of the AC voltage (the thyristor has to forward-bias before current can flow), and so current must lag the corresponding voltage. This results in lagging power factor operation on both rectifier and inverter sides. Therefore, LCC-based rectifier and inverter both are reactive sinks and require capacitive compensation.

For this reason, LCC terminal placement within an AC network is usually limited to only stiff buses, i.e., buses that have high short-circuit duty, in order to ensure that reactive power sources will be close and therefore capable of providing the reactive power necessary by the LCC terminals.

In contrast, because of its additional control capability, VSCs are able to both consume and supply reactive power. Thus, they are a voltage control device themselves, and therefore, their terminal locations need not be limited to only stiff

locations within the network. This is a decided benefit on the part of VSC-based HVDC.

The below table identified the two main types of HVDC by the typical names given to them.

Based on	Thyristor	IGBT
Commutation	LCC	
Source	CSC	VSC

From [6] (*italics added*),

“VSC converter technology can rapidly control both active and reactive power independently of one another. Reactive power can also be controlled at each terminal independent of the HVDC transmission voltage level. *This control capability gives total flexibility to place converters anywhere in the AC network since there is no restriction on minimum network short circuit capacity.* Forced commutation with VSC even permits black start, i.e., the converter can be used to synthesize a balanced set of three phase voltages like a virtual synchronous generator. *The dynamic support of the ac voltage at each converter terminal improves the voltage stability and increases the transfer capability of the sending and receiving end AC systems.*”

It is of interest that, at one time, VSC-based HVDC was referred to by ABB as “HVDC-Light,” in

contrast to the thyristor-based HVDC which they refer to as “HVDC-Classic.” On the other hand, Siemens called VSC-based HVDC by the name of HVDC^{PLUS}, where “PLUS” stands for “Power Link Universal Systems” [7]. Siemens also used “HVDC-Classic” to refer to thyristor-based HVDC. I am unsure if ABB and Siemens are still using this terminology.

The table below lists some HVDC-VSC implementations as of 2003 [8].

VSC Project	Rating	VSC Rationale
Hellsjön	3 MW, ±10 kV 10 km	Development
Hagfors	0-44 MVAR	EAF flicker mitigation
Gotland	50 MW, ±80 kV 70 km underground	- Wind power - Environmental - Voltage support - Stabilize AC lines
Tjæreborg	7 MW, ±10 kV 4 km underground	- Wind power testing - Variable frequency - Voltage support
Directlink	3 x 60 MW, ±80 kV 65 km underground	- Asynchronous Tie - Weak systems - Environmental - Permitting
Moselstahlwerk	0-38 MVAR	EAF flicker mitigation
Eagle Pass	36 MVA	- Weak system - Voltage support - Asynchronous Tie - Black start
Cross Sound Cable Intercon.	330 MW, ±150 kV 40 km submarine	- Controllability - System interface
Murray Link	200 MW, ±150kV 180km underground	- Asynchronous Tie - Weak systems - Environmental - Permitting
Polarit	0-164 MVAR	EAF flicker mitigation
Evron	0-36 MVAR	- Load balancing - Active filtering
Troll A	2 x 40 MW, ±60 kV 70 km submarine	- Offshore platform - Var. speed drive - Environmental - Black start
Holly	-80/+100 MVAR	- Voltage support - Retired generator - Cap bank control - Small site

Reference [9] lists examples of possible HVDC-Light applications as of 2005. Reference [10] is a more recent publication (pulled from the internet in 2021) showing 35 installations from Hitachi-ABB, below.

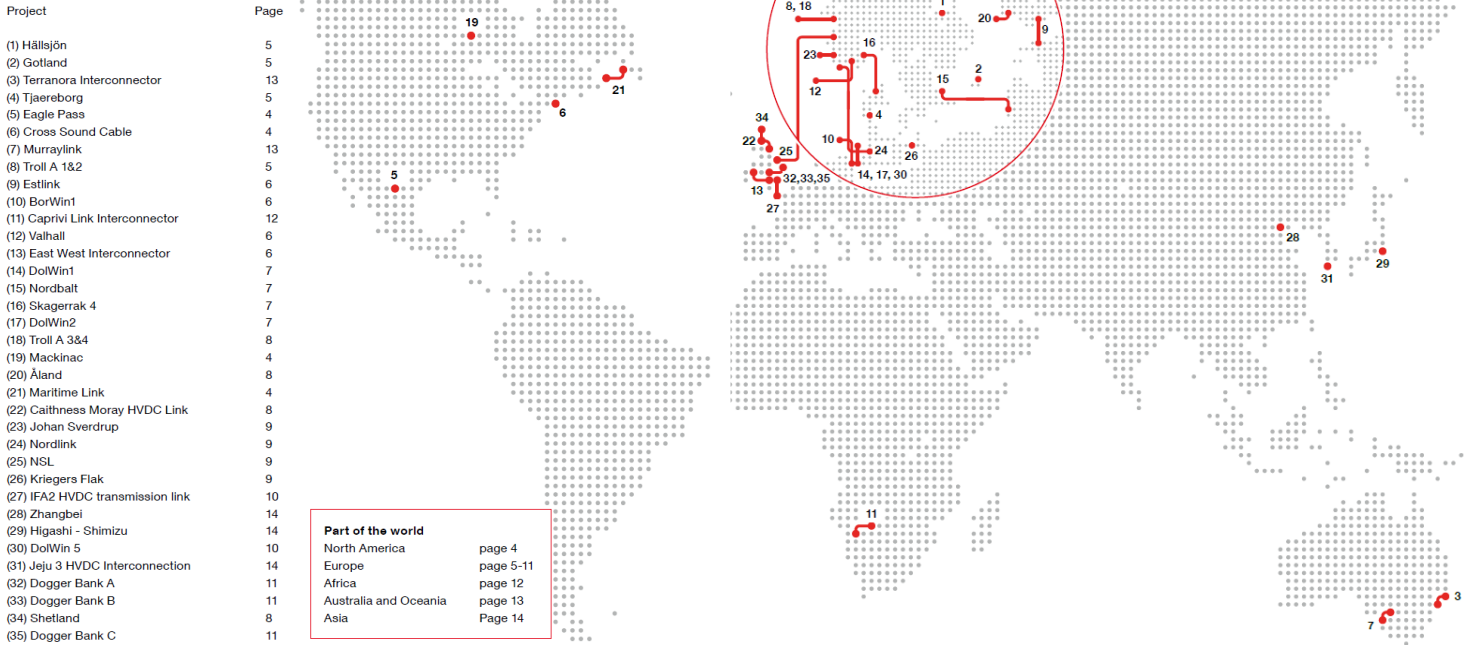


Figure 9e below contrasts Siemen’s experience with LCC-based HVDC (top) vs. VSC-based HVDC (bottom) [7].

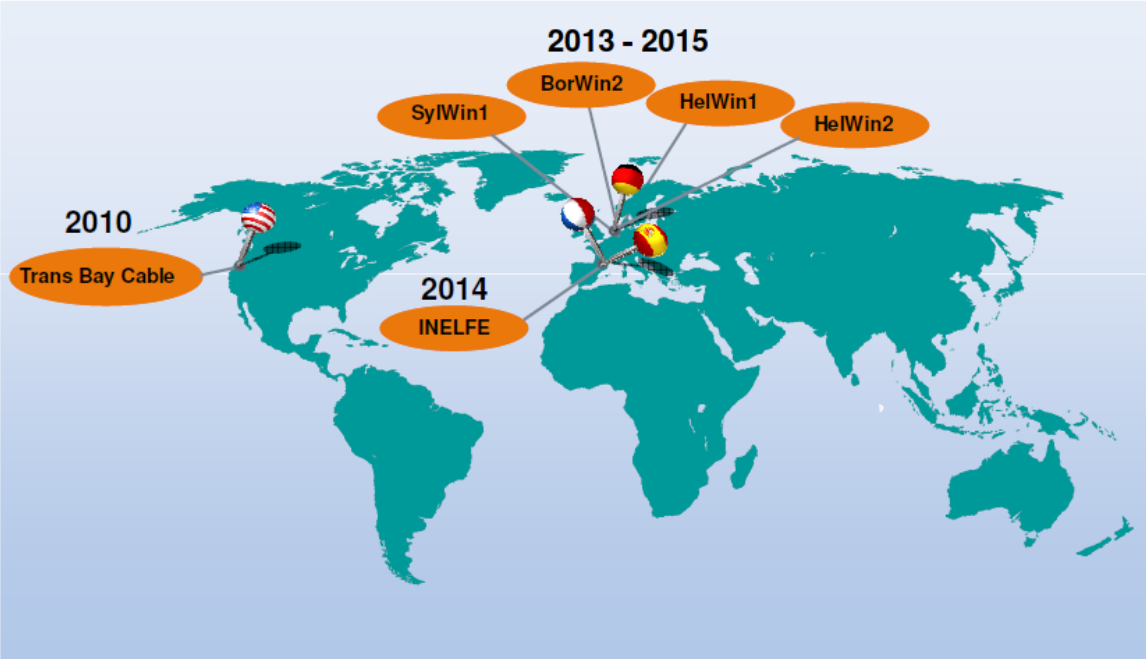
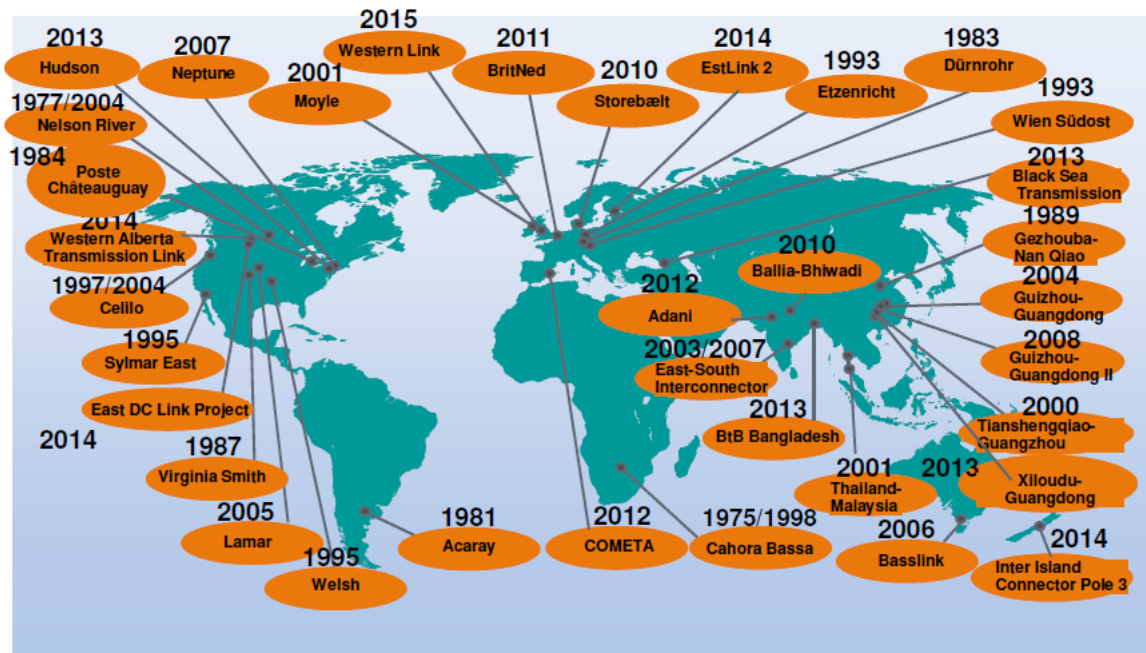


Fig. 9e

Reference [11], from 2019, identifies some more recent HVDC VSC projects, as indicated in the below table.

Table1 Recent typical VSC-HVDC projects

Name	Converter	Capacity/ MW	Voltage /kV	Year
British NEMO	VSC	1000	±400	2019
Denmark Viking	VSC	1400	±400	2022
Germany BorWin3	VSC	800	±300	2019
France FAB	VSC	1400	±320	2018
Zhangbei Demonstration Project	VSC	3000	±500	2022

Reference [8] summarizes applications of VSC, as follows:

- Point-to-point schemes—overhead lines
- Point-to-point schemes—cables
- In-feeds to city centers
- Transmission to/from weak ac systems
- Back-to-back schemes
- In parallel with an existing line-commutated converter (LCC) HVDC link, for increase of transfer capability
- **Enhancement of an ac system**
- As a parallel link to ac transmission lines, to reduce bottlenecks in transmission networks
- DC land cable systems
- DC transmission cables in areas where it is impossible to obtain overhead line permission.
- **Multi-terminal systems**
- **Connection to wind farms (onshore or offshore)**

- Interconnections of asynchronous power systems
- Supply of loads in isolated areas
- Supply to and from offshore loads/platforms

Reference [9] compares and contrasts VSC to thyristor-based converters, as follows.

Advantages of VSC over thyristor-based converters:

- The VSC valves are self-commutating.
- Commutation failures due to ac system fault or ac voltage dips do not occur.
- **The VSC may be operated at a very small short-circuit ratio (SCR).**
- **Reactive power, either capacitive or inductive, can be controlled independent of the active power within the rating of the equipment.**
- **Reactive shunt compensation is not required.**
- **The VSC stations can be operated as STATCOMs, even if the VSC is not connected to the dc line.**
- **The VSC can energize a passive or dead ac system.**
- Only harmonic filters are needed, and they need not be switchable.
- Depending on the converter topology, if transformers are needed they do not have to be specially-designed HVDC converter transformers, but conventional ac transformers may be used.

- The VSC control can be designed such that the VSC stations can eliminate flicker and selected harmonics in the ac system.
- The footprint of a VSC station is considerably smaller than an LCC HVDC station.
- Inherently, VSC Transmission can operate without telecommunication between the VSC substations.
- **The voltage polarity on the dc side is always the same. DC cables are always exposed to the same voltage polarity.**
- **DC line faults require opening of the VSC ac circuit breakers at both ends of a scheme in order to clear the dc fault, unless appropriate dc breakers are provided in the scheme.**

Reference [9] also lists disadvantages of VSC relative to thyristor-based converters:

- Practical experience with VSC Transmission is not as extensive as with LCC.
- Power handling capability is less than with LCC. For high transmission capacities, more parallel VSC transmission schemes are required than for LCC, which adds costs and losses to a VSC solution.
- The switching losses in the VSC valves are higher compared with similar LCC valves, primarily due to higher switching frequency, and because a VSC valve has many more semiconductor switches than an LCC valve of the same rating.

4.0 Multiterminal configurations

It is sometimes desirable to configure HVDC lines with more than one terminal. Multi-terminal HVDC (MTDC) represent a solution to the problem that HVDC suffers from no “on-ramps” between its terminals. However, additional terminals significantly increase the cost, relative to EHVAC solutions. MTDC configurations are desirable in order to provide such “on-ramps” as illustrated in Fig. 11.

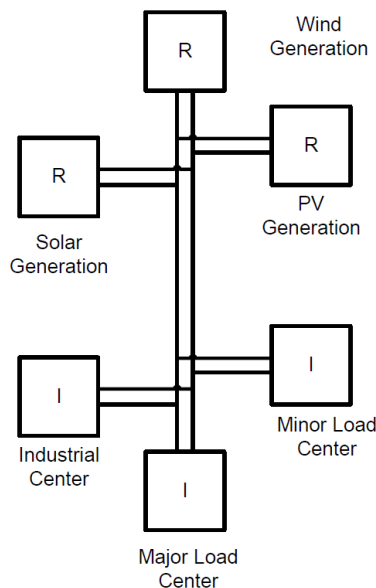
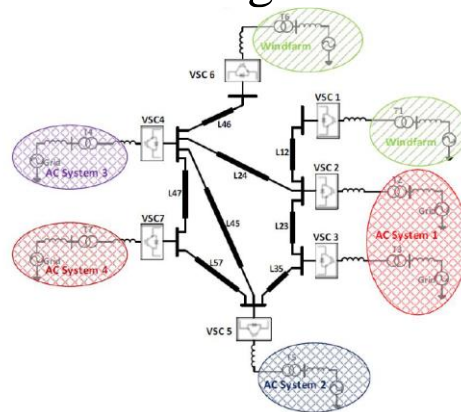


Fig. 11

The basic reason why multiterminal configurations can be implemented with VSC is associated with bus polarity.

LCC-based converters cannot do a current reversal, therefore in order to change power flow direction, it must do a voltage polarity change at the terminal to which it is connected. If this terminal has other

circuits connected to it, then that polarity change will also reverse the power flow in the other circuits. In contrast, VSC reverses the current in order to change power flow direction [12]. This has no impact on other DC circuits connected to the terminal (KCL can be satisfied from the AC side). The figure below shows a DC multi-terminal grid.



Therefore one must choose between: (a) two-terminals and no on-ramps; (b) multi-terminals with VSC and limited capacity.

There are two other issues regarding multiterminal connections.

1. Faults: DC faults are hard to interrupt because there is no natural current zero; thus, an HVDC circuit breaker must interrupt a very high current. With two-terminal HVDC, when a DC circuit is faulted, one may just interrupt the current on the AC side of the converter and still only affect the faulted circuit. With a MTDC system, however, interrupting the AC side connected to a DC bus

that is serving more than one circuit will affect both of those circuits. This is unacceptable from a reliability point of view. Thus, an HVDC circuit breaker has to create the zero current crossing. To do that, it injects a counter-voltage in the circuit, high enough to counteract the sources [13]. ABB announced that it had developed the “hybrid HVDC breaker” in 2012 [14], as shown in the figure below. Here, the current normally flows through the top path, but during fault conditions, the ultra-fast disconnecter detects di/dt and before it becomes too high, opens to shunt the current to the lower path. The reduced current through the high-impedance lower path can then be interrupted.

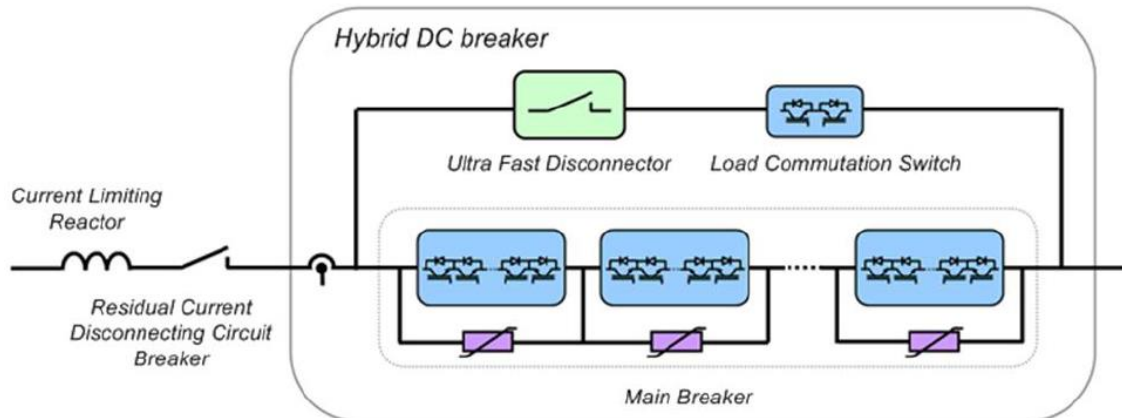


Figure 14 [14] illustrates an MTDC grid that was proposed for Europe. This design is not possible without VSC-based HVDC and HVDC breakers.

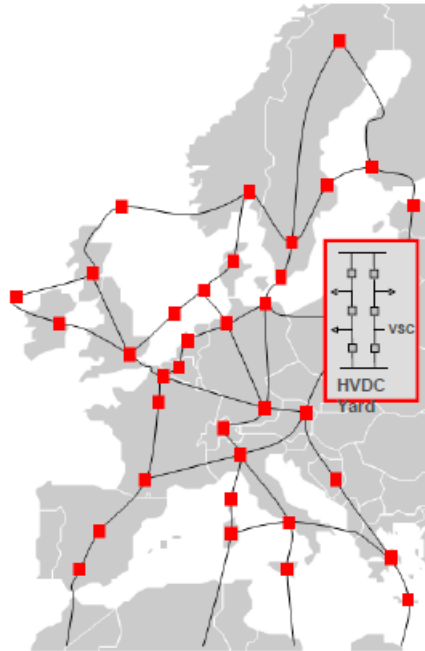


Fig. 14

2. Communications: When the flow from the AC side into a converter at one terminal changes, all other terminals have to know this in order to continue satisfying KCL into the DC system. This requires communication systems to coordinate.

Multi-terminal HVDC development in China

China has also been leading the development of multi-terminal HVDC projects. Two representative projects are the three terminal $\pm 800\text{kV}$, 8GW Wudongde HVDC grid, and the four terminal $\pm 500\text{kV}$ 3GW Zhangbei VSC-MTDC grid. The Wudongde HVDC grid is the first high capacity hybrid LCC-VSC HVDC grid in the world. The 1498km UHVDC line delivers hydro power from the Yunan province in the Southwest to Guangxi and Guangdong provinces in the east, as illustrated in Fig. 14a [15]. The

Zhangbei VSC-MTDC grid integrates various energy resources, such as wind, solar and pumped hydro in three sending stations, and delivers clean energy into the load center in Beijing, as shown in Fig. 14b [15].

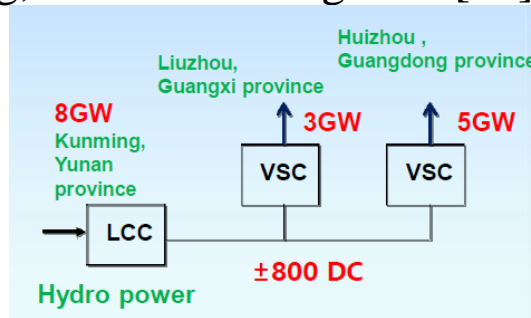


Figure 14a: Wudongde three terminal hybrid UHVDC grid [15]

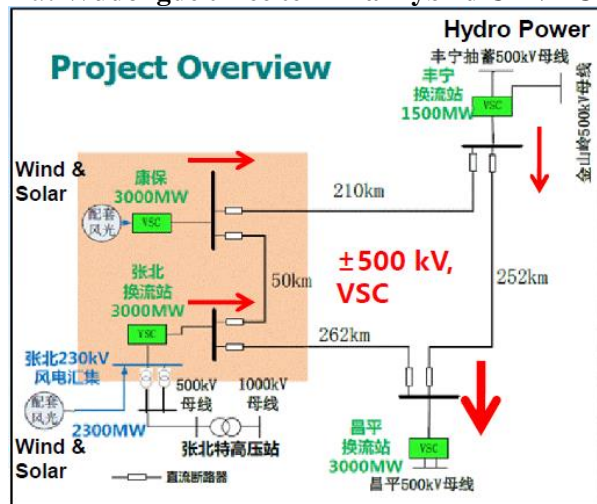


Figure 14b: Zhangbei VSC-HVDC grid [15]

5.0 Harmonics

We already mentioned that the 12-pulse bridge generates harmonic multiples of the fundamental frequency equal to $12n \pm 1$ where n equals all positive integers. Likewise, the 6-pulse bridge generates harmonic multiples of the fundamental frequency equal to $6n \pm 1$. This can be shown as follows.

Fig. Y below is an illustration of a converter, either a LCC or a VSC.

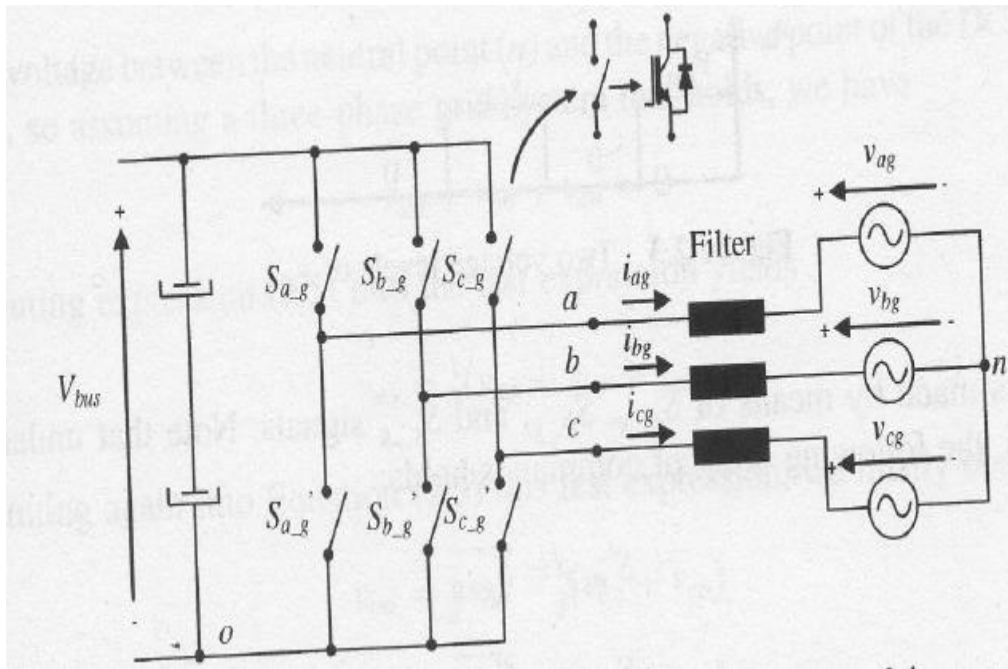


Fig. Y

The commands of the upper switches are made by signals S_{ag} , S_{bg} , and S_{cg} , and of the lower switches by signals S'_{ag} , S'_{bg} , and S'_{cg} . We will require, for any leg, that the state of the lower switch be opposite to the state of the upper switch, i.e.,

$$S'_{ag} = \bar{S}_{ag}; \quad S'_{bg} = \bar{S}_{bg}; \quad S'_{cg} = \bar{S}_{cg};$$

where the overbar means “complement.” (Without this requirement, two switches in the same leg could be closed simultaneously in which case it would short the DC voltage causing $V_{BUS}=0$.)

By inspecting the switching circuit of Fig. Y, we observe that the DC voltage V_{bus} is connected across phase a when $S_{ag}=1$ (closed), which necessarily

implies $S'_{ag}=0$. A similar thing can be said for the b-phase and for the c-phase. Noting the location of the point “o” on the DC bus low side, we may represent this according to:

$$v_{ao} = V_{bus} S_{ag} \quad S_{ag} \in \{0,1\}$$

$$v_{bo} = V_{bus} S_{bg} \quad S_{bg} \in \{0,1\}$$

$$v_{co} = V_{bus} S_{cg} \quad S_{cg} \in \{0,1\}$$

Generalizing the above results in

$$v_{jo} = V_{bus} S_{jg} \quad S_{jg} \in \{0,1\}, \quad j = a, b, c$$

We note that this converter may have two possible voltages for each phase, V_{bus} or 0; therefore it is referred to as a two-level converter. Multi-level converters are also used.

But now let's consider the phase voltages to neutral, where we note that the point “n” in Fig. Y is the AC bus neutral. Focusing on only the a-phase, we can draw Fig. Z below.

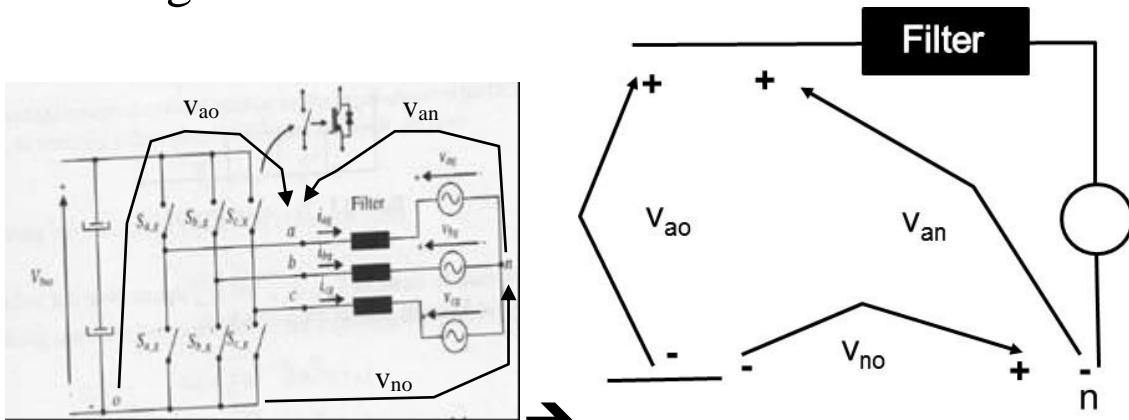


Fig. Z

From this, we can use KVL to derive

$$v_{an} = v_{ao} - v_{no}$$

$$v_{bn} = v_{bo} - v_{no}$$

$$v_{cn} = v_{co} - v_{no} \quad (*)$$

And from balanced phase voltages (same magnitude, separated in time by 120°) we have $v_{an} + v_{bn} + v_{cn} = 0$; substitution of the above three relations yields:

$$v_{no} = \frac{1}{3}(v_{ao} + v_{bo} + v_{co}) \quad (**)$$

Substitution of (**) into the 3 equations of (*) yields

$$v_{an} = v_{ao} - v_{no} = v_{ao} - \frac{1}{3}(v_{ao} + v_{bo} + v_{co}) = \frac{2}{3}v_{ao} - \frac{1}{3}(v_{bo} + v_{co})$$

$$v_{bn} = v_{bo} - v_{no} = v_{bo} - \frac{1}{3}(v_{ao} + v_{bo} + v_{co}) = \frac{2}{3}v_{bo} - \frac{1}{3}(v_{ao} + v_{co})$$

$$v_{cn} = v_{co} - v_{no} = v_{co} - \frac{1}{3}(v_{ao} + v_{bo} + v_{co}) = \frac{2}{3}v_{co} - \frac{1}{3}(v_{ao} + v_{bo})$$

Then use (from previous)

$$v_{ao} = V_{bus} S_{ag}$$

$$v_{bo} = V_{bus} S_{bg}$$

$$v_{co} = V_{bus} S_{cg}$$

Substitution yields our phase/switch equations:

$$v_{an} = \frac{2}{3}v_{ao} - \frac{1}{3}(v_{bo} + v_{co}) = \frac{2}{3}V_{bus} S_{ag} - \frac{1}{3}(V_{bus} S_{bg} + V_{bus} S_{cg}) = \frac{V_{bus}}{3}(2S_{ag} - S_{bg} - S_{cg})$$

$$v_{bn} = \frac{2}{3}v_{bo} - \frac{1}{3}(v_{ao} + v_{co}) = \frac{2}{3}V_{bus} S_{bg} - \frac{1}{3}(V_{bus} S_{ag} + V_{bus} S_{cg}) = \frac{V_{bus}}{3}(2S_{bg} - S_{ag} - S_{cg})$$

$$v_{cn} = \frac{2}{3}v_{co} - \frac{1}{3}(v_{ao} + v_{bo}) = \frac{2}{3}V_{bus} S_{cg} - \frac{1}{3}(V_{bus} S_{ag} + V_{bus} S_{bg}) = \frac{V_{bus}}{3}(2S_{cg} - S_{ag} - S_{bg})$$

Now we have expressed our line-to-neutral voltages in terms of switch statuses.

How many different combinations of switches do we have? We need specify only the top three switches as each top switch determines the status of the bottom switch via the complementary operation. Therefore, we have the following switch combinations:

000, 001, 010, 011, 100, 101, 110, 111

We will call these “switch states.” We can observe the converter configuration for the different switch states in Fig. W.

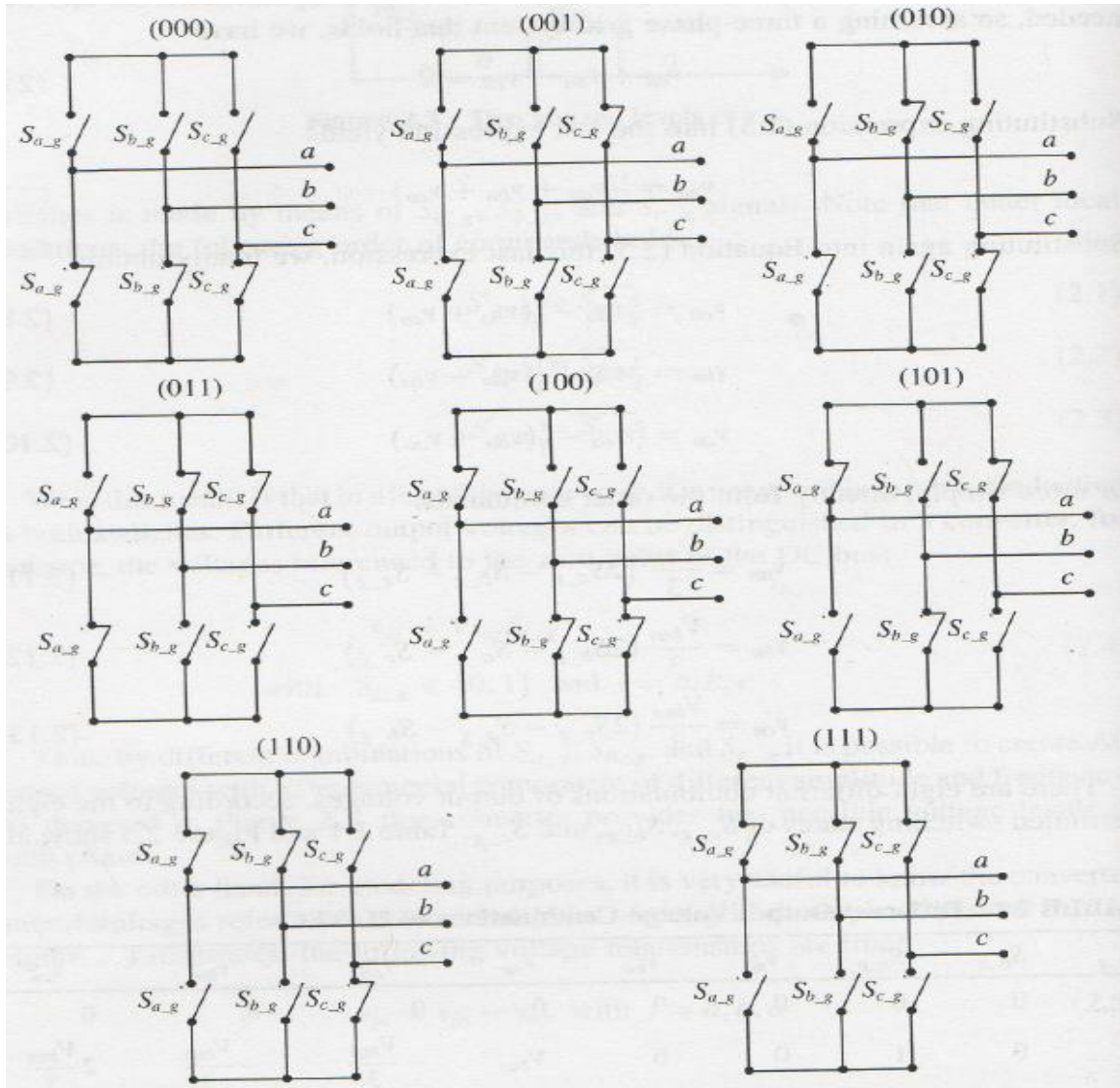


Fig. W

Lets evaluate our phase/switch equations for each switch status. For example, for 000:

$$v_{an} = \frac{V_{bus}}{3} (2S_{ag} - S_{bg} - S_{cg}) = 0$$

$$v_{bn} = \frac{V_{bus}}{3} (2S_{bg} - S_{ag} - S_{cg}) = 0$$

$$v_{cn} = \frac{V_{bus}}{3} (2S_{cg} - S_{ag} - S_{bg}) = 0$$

Or for 001:

$$v_{an} = \frac{V_{bus}}{3}(0-0-1) = -\frac{V_{bus}}{3}$$

$$v_{bn} = \frac{V_{bus}}{3}(0-0-1) = -\frac{V_{bus}}{3}$$

$$v_{cn} = \frac{V_{bus}}{3}(2(1)-0-0) = \frac{2V_{bus}}{3}$$

The following table provides switch status, v_{jo} , and v_{jn} for all eight states.

TABLE 2.1 Different Output Voltage Combinations of 2L-VSC

S_{a_g}	S_{b_g}	S_{c_g}	v_{ao}	v_{bo}	v_{co}	v_{an}	v_{bn}	v_{cn}
0	0	0	0	0	0	0	0	0
0	0	1	0	0	V_{bus}	$-\frac{V_{bus}}{3}$	$-\frac{V_{bus}}{3}$	$2\frac{V_{bus}}{3}$
0	1	0	0	V_{bus}	0	$-\frac{V_{bus}}{3}$	$2\frac{V_{bus}}{3}$	$-\frac{V_{bus}}{3}$
0	1	1	0	V_{bus}	V_{bus}	$-2\frac{V_{bus}}{3}$	$\frac{V_{bus}}{3}$	$\frac{V_{bus}}{3}$
1	0	0	V_{bus}	0	0	$2\frac{V_{bus}}{3}$	$-\frac{V_{bus}}{3}$	$-\frac{V_{bus}}{3}$
1	0	1	V_{bus}	0	V_{bus}	$\frac{V_{bus}}{3}$	$-2\frac{V_{bus}}{3}$	$\frac{V_{bus}}{3}$
1	1	0	V_{bus}	V_{bus}	0	$\frac{V_{bus}}{3}$	$\frac{V_{bus}}{3}$	$-2\frac{V_{bus}}{3}$
1	1	1	V_{bus}	V_{bus}	V_{bus}	0	0	0

Notice that v_{jo} takes only two different voltage levels, but v_{an} takes five different voltage levels.

Let's now order the switching states as follows:

- t_1 110
- t_2 100
- t_3 101
- t_4 001
- t_5 011
- t_6 010

This is our six pulse generation scheme.

Now compute the resulting v_{jn} outputs using our phase/switch equations:

$$v_{an} = \frac{V_{bus}}{3} (2S_{ag} - S_{bg} - S_{cg})$$

$$v_{bn} = \frac{V_{bus}}{3} (2S_{bg} - S_{ag} - S_{cg})$$

$$v_{cn} = \frac{V_{bus}}{3} (2S_{cg} - S_{ag} - S_{bg})$$

And plotting the switch statuses together with the line-to-neutral voltages, we observe Fig. V below.

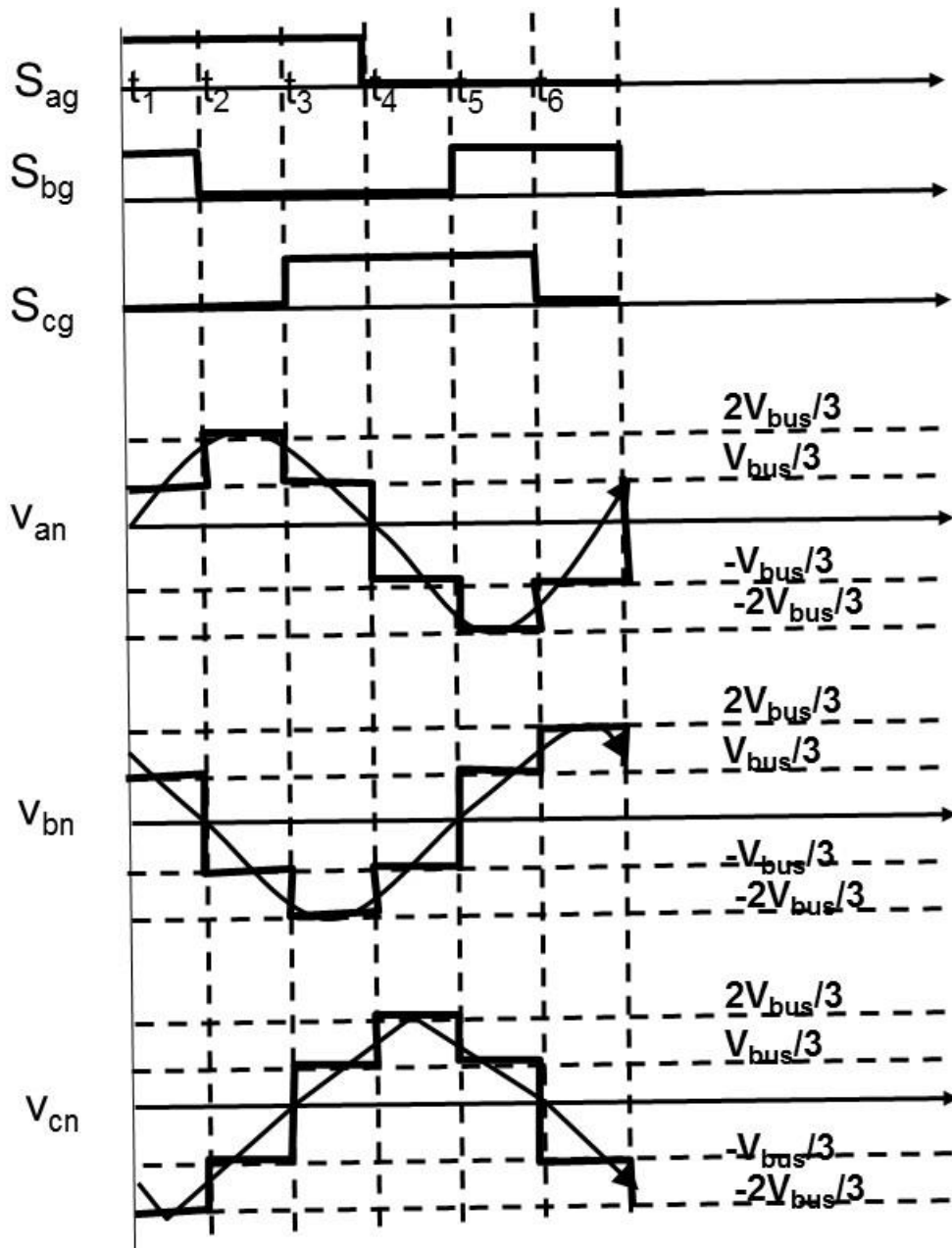


Fig. V

The waveforms of Fig. V are AC voltages, and these are the voltages that are injected into the AC system by the converter. We can obtain the Fourier series of this function according to

$$f(t) = a_0 + \sum_{n=1}^{\infty} a_n \cos n\omega_0 t + b_n \sin n\omega_0 t$$

where

$$a_0 = \frac{1}{T_0} \int_{T_0} f(t) dt$$

$$a_n = \frac{2}{T_0} \int_{T_0} f(t) \cos n\omega_0 t dt$$

$$b_n = \frac{2}{T_0} \int_{T_0} f(t) \sin n\omega_0 t dt$$

Observe $v_{an}(t)$ in Fig. V; it has the following attributes:

- This function is half-wave symmetric, $f(t-T_0/2)=-f(t)$
→ even harmonics $n=0,2,4,\dots$ do not exist
- It is also an odd function (symmetric about the origin) and therefore

$$a_n = 0; \quad b_n = \frac{4}{T_0} \int_0^{T_0/2} f(t) \sin n\omega_0 t dt$$

So let's compute the b_n coefficient for v_{an} .

$$\begin{aligned} b_n &= \frac{4}{T_0} \int_0^{T_0/2} f(t) \sin n\omega_0 t dt \\ &= \frac{4}{T_0} \left\{ \int_0^{T_0/6} \frac{V_{bus}}{3} \sin n\omega_0 t dt + \int_{T_0/6}^{T_0/3} \frac{2V_{bus}}{3} \sin n\omega_0 t dt + \int_{T_0/3}^{T_0/2} \frac{V_{bus}}{3} \sin n\omega_0 t dt \right\} \\ &= \frac{-4}{T_0} \frac{V_{bus}}{3n\omega_0} \left\{ \cos n\omega_0 t \Big|_0^{T_0/6} + 2 \cos n\omega_0 t \Big|_{T_0/6}^{T_0/3} + \cos n\omega_0 t \Big|_{T_0/3}^{T_0/2} \right\} \\ &= \frac{-4}{T_0} \frac{V_{bus} T_0}{3n2\pi} \left\{ \left(\cos n \frac{2\pi}{T_0} \frac{T_0}{6} - 1 \right) + 2 \left(\cos n \frac{2\pi}{T_0} \frac{T_0}{3} - \cos n \frac{2\pi}{T_0} \frac{T_0}{6} \right) + \left(\cos n \frac{2\pi}{T_0} \frac{T_0}{2} - \cos n \frac{2\pi}{T_0} \frac{T_0}{3} \right) \right\} \\ &= \frac{-2V_{bus}}{3n\pi} \left\{ \cos n \frac{\pi}{3} - 1 + 2 \cos n \frac{2\pi}{3} - 2 \cos n \frac{\pi}{3} + \cos n\pi - \cos n \frac{2\pi}{3} \right\} \\ &= \frac{-2V_{bus}}{3n\pi} \left\{ -\cos n \frac{\pi}{3} - 1 + \cos n \frac{2\pi}{3} - 1 \right\} = \frac{-2V_{bus}}{3n\pi} \left\{ -2 - \cos n \frac{\pi}{3} + \cos n \frac{2\pi}{3} \right\} \\ &= \frac{2V_{bus}}{3n\pi} \left\{ 2 + \cos n \frac{\pi}{3} - \cos n \frac{2\pi}{3} \right\} \end{aligned}$$

Observe that harmonics of multiples of 3 also do not exist, since for $n=3,6,9,\dots$

$$2 + \cos n \frac{\pi}{3} - \cos n \frac{2\pi}{3} = 2 - 1 - 1 = 0 \quad \Rightarrow b_n = 0$$

Therefore, only $n=1, 5, 7, 11, 13, 17, 19, 23, 25, 29, \dots$ exist, which conforms to harmonic multiples of the fundamental frequency equal to $6n \pm 1$.

-
- [1] K. Padiyar, "HVDC Power Transmission Systems," New Academic Science, second edition, 2011.
- [2] M. El-Sharkawi, "Fundamentals of Electric Drives," Brooks/Cole Publishing, 2000.
- [3] D. Woodford, "HVDC Transmission," a white paper written for Manitoba HVDC Research Centre, 1998.
- [4] M. Szechtman, M. Zavahir, and J. Jyrinsalo, "The role of SC B4 – HVDC and Power Electronics in Developing the Power Grid for the Future," Electra, June 2008.
- [5] A. Yazdani and R. Iravani, "Voltage-sourced converters in power systems: modeling, control, and applications," Wiley, 2010.
- [6] M. Bahrman, "Overview of HVDC Transmission," Proc of the 2006 PSCE.
- [7] P. Kohnstam, "High voltage direct current transmission," Presentation slides to the US DOE, April 22, 2013, available at http://energy.gov/sites/prod/files/2013/05/f0/HVDC2013-Kohnstam_0.pdf.
- [8] M. Bahrman, J. Johansson, and B. Neilsen, "Voltage source converter transmission technologies: the right fit for the right application," Proc. of the 2003 IEEE Power Engineering Society General Meeting, July 3-17, 2003.

-
- [9] “VSC Transmission, CIGRE, 2005.
- [10] “HVDC Light – The original VSC technology,” a Hitachi-ABB publication available at <https://search.abb.com/library/Download.aspx?DocumentID=POW0027&LanguageCode=en&DocumentPartId=&Action=Launch>.
- [11] R. Jiao, J. Ding, J. Ren, Lianing Lv, and X. Chen, “Analysis and Simulation of New DC Power Grids for Large-scale Clean Energy Integration and Transmission,” 8th Renewable Power Generation Conference (RPG 2019), Shanghai, China, 2019, pp. 1-6, doi: 10.1049/cp.2019.0356.
- [12] M. Bahrman and B. Johnson, “The ABCs of HVDC Transmission Technologies: An Overview of High Voltage Direct Current Systems and Applications,” IEEE Power and Energy Magazine, March/April 2007.
- [13] V. Lescale, A. Kumar, L. Juhlin, H. Bjorklund, and K. Nyberg, “Challenges with multi-terminal UHVDC transmissions,” Power India Conference, Oct 12-15, 2008, New Delhi, India.
- [14] M. Callavik, A. Blomberg, J. Hafner, and B. Jacobson, “The hybrid HVDC breaker: an innovation breakthrough enabling reliable HVDC grids,” 2012, available at http://new.abb.com/docs/default-source/default-document-library/hybrid-hvdc-breaker---an-innovation-breakthrough-for-reliable-hvdc-gridsnov2012finmc20121210_clean.pdf?sfvrsn=2.
- [15] L. Yao, “DC Grid with DC/DC Converters – Alaboratory Demonstrator,” IEEE PES HVDC WG 15.05.02 meeting